Supporting Information for Classification and quantitative characterisation of the excited states of π-conjugated diradicals

Lujo Matasović,[†] Hugo Bronstein,[‡] Richard H. Friend,[†] and Felix Plasser[*,¶]

†*Cavendish Laboratory, University of Cambridge, Cambridge, UK*

‡*Yusuf Hamied Department of Chemistry, University of Cambridge, Cambridge, UK*

¶*Department of Chemistry, Loughborough University, Loughborough, LE11 3TU, United Kingdom*

E-mail: f.plasser@lboro.ac.uk

Phone: +44 1509 226946

S1 – Derivation of descriptors

In this section we sketch the derivation of the values of the wave function descriptors within the two-orbital two-electron model. As described in the main text, we consider the four states:

$$|\Psi_0\rangle = \cos(\eta)|\phi_H\bar{\phi}_H\rangle - \sin(\eta)|\phi_L\bar{\phi}_L\rangle \tag{1}$$

$$|\Psi_T\rangle = \frac{1}{\sqrt{2}}\left(|\phi_H\bar{\phi}_L\rangle - |\phi_L\bar{\phi}_H\rangle\right) \tag{2}$$

$$|\Psi_Z\rangle = \frac{1}{\sqrt{2}}\left(|\phi_H\bar{\phi}_L\rangle + |\phi_L\bar{\phi}_H\rangle\right) \tag{3}$$

$$|\Psi_1\rangle = \sin(\eta)|\phi_H\bar{\phi}_H\rangle + \cos(\eta)|\phi_L\bar{\phi}_L\rangle \tag{4}$$

We start by finding the matrix representation of the one-electron transition densities for each excited state with respect to the ground state Ψ_0. Using the creation and annihilation operators referring to orbitals ϕ_p and ϕ_q we can write for a general matrix element:

$$D^{0J}_{pq} = \langle\Psi_0|a^\dagger_p a_q|\Psi_J\rangle \tag{5}$$

where p and q refer to $H, \bar{H}, L$ and $\bar{L}$ orbitals. The spin-traced transition densities read:

$$\mathbf{D}^{01} = \frac{\sin 2\eta}{\sqrt{2}}\begin{pmatrix} 1 & 0 \\ 0 & -1 \end{pmatrix} \tag{6}$$

$$\mathbf{D}^{0Z} = \begin{pmatrix} 0 & \cos\eta \\ -\sin\eta & 0 \end{pmatrix} \tag{7}$$

$$\mathbf{D}^{0T} = \begin{pmatrix} 0 & -\cos\eta \\ -\sin\eta & 0 \end{pmatrix} \tag{8}$$

Note that a factor $\sqrt{2}$ has been absorbed into these expressions to account for the separate $\alpha\alpha$ and $\beta\beta$ contributions. Squaring the norm of calculated densities, we acquire the one-electron excitation character, Ω:

$$\Omega^{01} = \|\mathbf{D}^{01}\|^2 = \sin^2 2\eta \tag{9}$$

$$\Omega^{0T} = \|\mathbf{D}^{0T}\|^2 = \Omega^{0Z} = \|D^{0Z}\|^2 = \sin^2\eta + \cos^2\eta = 1 \tag{10}$$

Next we compute the particle-hole permutation operator expectation values for each transition of interest:

$$\langle P_{he}\rangle^{0J} = \frac{1}{\Omega^{0J}} \sum_{pq} D_{pq} D_{qp} \tag{11}$$

$$\langle P_{he}\rangle^{01} = 1 \tag{12}$$

$$\langle P_{he}\rangle^{0T} = \sin\eta\cos\eta + \cos\eta\sin\eta = \sin 2\eta \tag{13}$$

$$\langle P_{he}\rangle^{0Z} = -\sin\eta\cos\eta - \cos\eta\sin\eta = -\sin 2\eta \tag{14}$$

In a similar fashion, we calculate the spin-traced one-electron density matrix for each state:

$$\mathbf{D}^{00} = 2\begin{pmatrix} \cos^2\eta & 0 \\ 0 & \sin^2\eta \end{pmatrix} \tag{15}$$

$$\mathbf{D}^{11} = 2\begin{pmatrix} \sin^2\eta & 0 \\ 0 & \cos^2\eta \end{pmatrix} \tag{16}$$

$$\mathbf{D}^{ZZ} = D^{TT} = \begin{pmatrix} 1 & 0 \\ 0 & 1 \end{pmatrix} \tag{17}$$

These are diagonal, meaning that the orbitals are already natural orbitals. We can, thus, directly obtain the number of unpaired electrons as:

$$n^0_{u,nl} = n^1_{u,nl} = (4\cos^4\eta\left(2 - 2\cos^2\eta\right)^2 + 4\sin^4\eta\left(2 - 2\sin^2\eta\right)^2) = 2\sin^4(2\eta) \tag{18}$$

$$n^T_{u,nl} = n^Z_{u,nl} = 2 \tag{19}$$

Next, we calculate difference density matrices:

$$\mathbf{D}_{\Delta}^{0Z} = \mathbf{D}_{\Delta}^{0T} = \begin{pmatrix} 1 - 2\cos^2\eta & 0 \\ 0 & 1 - 2\sin^2\eta \end{pmatrix} \tag{20}$$

$$\mathbf{D}_{\Delta}^{01} = 2 \begin{pmatrix} \sin^2\eta - \cos^2\eta & 0 \\ 0 & \cos^2\eta - \sin^2\eta \end{pmatrix} \tag{21}$$

The promotion numbers are equivalent to one of the diagonal elements, since the matrix is diagonal and already has two entries (one for attachment and one for detachment)

$$p^{01} = 2(\cos^2\eta - \sin^2\eta) = 2\cos 2\eta \tag{22}$$

$$p^{0T} = p^{0Z} = 1 - 2\sin^2\eta \tag{23}$$

Finally, we note for the transition dipole moment, e.g., its x-component:

$$\mu_x^{OZ} = \mu_x^{HL}\cos\eta - \mu_x^{HL}\sin\eta = \mu_x^{HL}(\cos\eta - \sin\eta) \tag{24}$$

$$(\mu_x^{OZ})^2 = (\mu_x^{HL})^2(\cos\eta - \sin\eta)^2 = (\mu_x^{HL})^2(1 - \sin 2\eta) \tag{25}$$

where μ_x^{HL} is the x-component of the dipole moment integral between ϕ_H and ϕ_L. Analogous equations hold for the y- and z-components. The oscillator strength is given as

$$f^{0Z} = \frac{2}{3}\Delta E^{0Z}[(\mu_x^{HL})^2 + (\mu_y^{HL})^2 + (\mu_z^{HL})^2] \tag{26}$$

If we approximate the energy gap (ΔE^{0Z}) and μ_x^{HL} as being constant, then we obtain:

$$f^{0Z} = f_0(1 - \sin 2\eta) \tag{27}$$

$$f_0 = \frac{2}{3}\Delta E^{0Z}[(\mu_x^{HL})^2 + (\mu_y^{HL})^2 + (\mu_z^{HL})^2] \tag{28}$$

S2 – Computational details

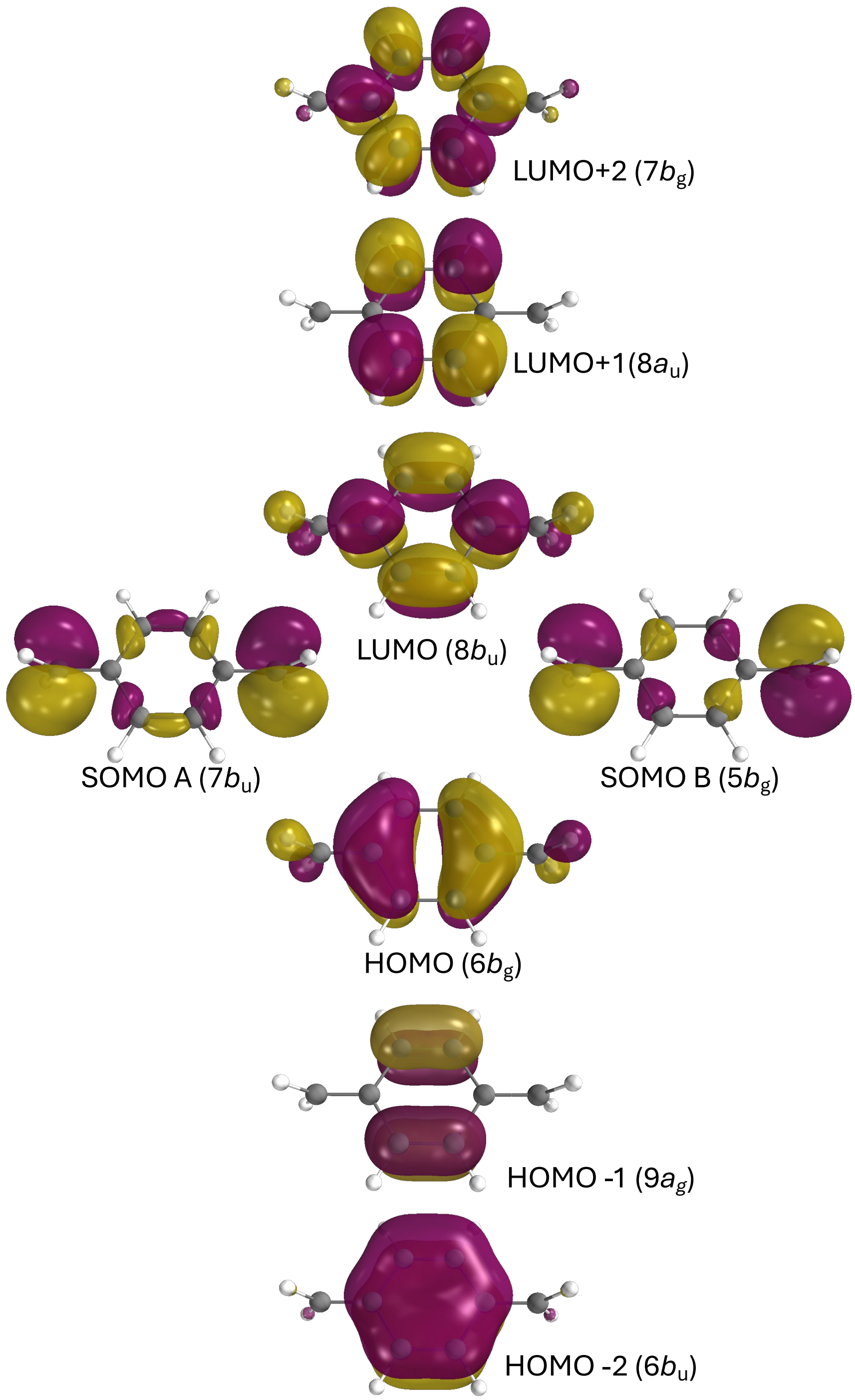

Figure S1: Orbitals in the active space for the CASSCF(8,8) computations performed.

S3 – Descriptors of all states at CASSCF level of theory

Table S1: Analysis of the excited states of pQDM at the planar geometry ($\theta = 0°$): vertical excitation energies (ΔE, eV), oscillator strengths (f) and wave function descriptors, calculated at CASSCF level of theory.

$\theta = 0°$							
State	ΔE	f	Ω	P_{he}	R_{he}	$n_{u,nl}$	p
1^1A_g	0.000	-	-	-	-	0.316	-
1^3A_u	2.047	-	0.940	0.556	0.501	2.220	1.050
1^3A_g	4.279	-	0.857	0.301	0.595	2.660	0.968
2^1A_g	4.764	-	0.383	0.322	-0.011	2.780	1.396
2^3A_u	5.079	-	0.870	0.302	0.426	2.722	1.101
3^3A_u	6.356	-	0.433	0.212	0.472	3.731	1.454
1^1A_u	6.633	1.214	0.839	-0.400	-0.062	2.079	1.043
2^3A_g	7.469	-	0.096	0.221	0.543	4.305	1.903
2^1A_u	7.631	0.044	0.370	0.105	0.158	3.430	1.464
3^1A_g	7.699	-	0.057	0.422	-0.577	4.230	1.837
4^3A_u	8.071	-	0.341	0.055	-0.035	3.886	1.653
3^3A_g	8.546	-	0.741	-0.007	-0.304	2.593	0.973
4^1A_g	9.18	-	0.154	-0.175	0.180	4.344	1.721
5^1A_g	9.221	-	0.745	-0.373	0.389	2.824	1.087
4^3A_g	9.379	-	0.242	0.109	0.231	4.522	1.951
5^3A_u	9.539	-	0.022	0.009	0.012	5.174	2.186
3^1A_u	9.748	0.829	0.863	-0.197	0.037	2.445	1.232
6^1A_g	10.204	-	0.331	0.060	-0.128	3.669	1.520
4^1A_u	10.835	0.051	0.588	-0.070	-0.381	2.872	1.227
6^3A_u	10.963	-	0.144	0.067	-0.288	4.576	1.859
7^1A_g	10.995	-	0.295	0.331	-0.589	3.852	1.684
5^3A_g	11.148	-	0.025	0.0530	-0.257	4.120	1.902
5^1A_u	11.566	0.0410	0.743	-0.301	0.410	2.801	1.245
6^3A_g	11.782	-	0.0250	0.136	0.003	5.367	2.343
6^1A_u	12.687	0.022	0.495	-0.016	0.160	3.243	1.418
8^1A_g	12.888	-	0.028	0.470	-0.267	4.028	1.787

Table S2: Analysis of the excited states of pQDM at the twisted geometry ($\theta = 90°$): vertical excitation energies (ΔE, eV), oscillator strengths (f) and wave function descriptors, at the CASSCF level of theory.

$\theta = 90°$							
State	ΔE	f	Ω	P_{he}	R_{he}	$n_{u,nl}$	p
1^3A_u	-0.151	-	0.995	0.995	0.814	2.214	0.239
1^1A_g	0.000	-	-	-	-	2.197	-
2^3A_u	2.784	-	0.969	0.515	0.324	4.156	1.105
1^3A_g	2.925	-	0.000	-0.073	0.233	4.157	1.048
2^1A_g	3.059	-	0.000	0.491	0.103	4.157	0.955
3^3A_u	4.912	-	0.822	0.233	0.200	4.346	1.192
1^1A_u	5.003	-	0.444	-0.003	0.232	2.127	1.129
2^3A_g	5.046	-	0.000	0.839	0.701	4.316	1.131
3^1A_g	5.258	-	0.000	0.654	-0.343	4.338	1.036
4^3A_u	5.381	-	0.441	0.003	0.212	2.121	1.142
4^1A_g	5.449	-	0.405	-0.006	0.260	2.143	1.030
3^3A_g	5.671	-	0.403	0.008	0.242	2.131	1.133
5^3A_u	6.269	-	0.000	0.091	0.025	5.126	1.380
4^3A_g	6.329	-	0.649	0.194	0.382	5.1	1.307
6^3A_u	6.587	-	0.000	0.135	0.019	4.966	1.594
2^1A_u	6.700	-	0.443	-0.002	0.189	2.108	1.139
5^1A_g	6.730	-	0.397	0.160	-0.110	4.948	1.393
5^3A_g	6.827	-	0.402	-0.001	0.203	2.118	1.129
3^1A_u	6.892	0.001	0.002	-0.403	-0.142	5.036	1.314
6^1A_g	6.997	-	0.406	-0.001	0.212	2.119	1.044
6^3A_g	7.229	-	0.000	0.186	0.082	4.102	0.984
4^1A_u	7.503	0.383	0.871	-0.377	-0.151	3.801	1.072
5^1A_u	7.803	0.068	0.766	-0.934	-0.759	2.346	0.509
7^1A_g	8.216	-	0.768	1.000	-0.803	2.329	0.235
8^1A_g	8.685	-	0.248	0.001	0.001	3.271	1.356
6^1A_u	8.747	-	0.220	-0.001	0.008	3.291	1.450
9^1A_g	10.082	-	0.001	0.085	-0.177	6.552	1.768

S4 – Descriptors of all states at MS-CASPT2 level of theory

Table S3: Analysis of the excited states of pQDM at the planar geometry ($\theta = 0°$): vertical excitation energies (ΔE, eV), oscillator strengths (f) and wave function descriptors.

			$\theta = 0°$				
State	ΔE	f	Ω	P_{he}	R_{he}	$n_{u,nl}$	p
1^1A_g	0.000	-	-	-	-	0.142	-
1^3A_u	2.279	0.000	0.930	0.381	0.353	2.153	1.128
1^3A_g	4.712	0.000	0.863	0.253	0.520	2.615	1.113
1^1A_u	4.784	1.447	0.843	-0.265	-0.048	2.067	1.156
2^1A_g	4.889	0.000	0.465	0.113	-0.121	2.838	1.405
2^3A_u	5.363	0.000	0.886	0.315	0.352	2.677	1.232
2^3A_g	6.639	0.000	0.822	0.063	-0.282	2.575	1.033
3^3A_u	6.993	0.000	0.468	0.168	0.397	3.697	1.542
3^1A_g	7.045	0.000	0.897	-0.316	0.351	2.596	1.048
4^1A_g	7.312	0.000	0.241	0.133	-0.451	3.397	1.622
2^1A_u	7.508	0.191	0.579	-0.045	0.021	3.107	1.395
3^1A_u	7.673	0.494	0.777	-0.238	0.060	2.870	1.329
3^3A_g	7.838	0.000	0.044	0.139	0.532	4.255	2.062
4^3A_u	8.047	0.000	0.390	0.054	0.061	3.746	1.657
5^1A_g	8.909	0.000	0.160	0.155	-0.311	4.174	1.899
4^1A_u	9.086	0.018	0.632	-0.034	-0.369	2.925	1.306
5^1A_u	9.378	0.006	0.813	-0.253	0.436	2.631	1.266
6^1A_g	9.506	0.000	0.014	0.264	-0.309	4.298	2.011
4^3A_g	9.542	0.000	0.078	0.128	0.067	4.223	1.939
5^3A_g	9.858	0.000	0.232	0.103	0.275	4.527	1.960
5^3A_u	10.111	0.000	0.024	-0.034	-0.298	5.168	2.241
6^1A_u	10.380	0.004	0.324	0.070	0.009	3.335	1.681
7^1A_g	10.694	0.000	0.043	0.112	-0.316	4.443	1.983
6^3A_u	10.977	0.000	0.072	0.067	-0.218	4.837	2.103
8^1A_g	11.008	0.000	0.141	0.079	-0.383	4.571	1.839
6^3A_g	12.251	0.000	0.024	0.155	0.078	5.370	2.420

Table S4: Analysis of the excited states of pQDM at the twisted geometry ($\theta = 90°$): vertical excitation energies (ΔE, eV), oscillator strengths (f) and wave function descriptors.

$\theta = 90°$							
State	ΔE	f	Ω	P_{he}	R_{he}	$n_{u,nl}$	p
1^1A_g	0.000	-	-	-	-	2.172	-
1^3A_u	0.118	0.000	0.993	0.992	0.810	2.207	0.294
2^1A_g	3.354	0.000	0.000	-	-	4.131	1.001
1^3A_g	3.411	0.000	0.000	-	-	4.131	1.101
2^3A_u	3.469	0.000	0.948	0.483	0.306	4.130	1.154
1^1A_u	3.622	0.000	0.465	0.007	0.242	2.128	1.123
3^3A_u	3.789	0.000	0.454	0.003	0.204	2.121	1.177
3^1A_g	3.935	0.000	0.397	0.004	0.278	2.145	1.046
2^3A_g	3.970	0.000	0.386	-0.002	0.235	2.131	1.178
4^1A_g	4.613	0.000	0.764	1.000	-0.797	2.316	0.327
2^1A_u	4.691	0.000	0.754	-0.972	-0.776	2.331	0.341
3^1A_u	4.854	0.000	0.465	-0.012	0.201	2.110	1.131
5^1A_g	5.026	0.000	0.395	-0.011	0.214	2.117	1.063
4^3A_u	5.161	0.000	0.832	0.251	0.216	4.309	1.233
6^1A_g	5.162	0.000	0.000	-	-	4.295	1.067
3^3A_g	5.180	0.000	0.385	0.008	0.196	2.118	1.161
4^3A_g	5.188	0.000	0.000	-	-	4.282	1.173
5^3A_g	5.540	0.000	0.000-	-	4.102	1.024	
4^1A_u	5.650	0.349	0.889	-0.331	-0.086	4.061	1.031
5^1A_u	6.727	0.000	0.000	-	-	5.041	1.311
6^3A_g	6.801	0.000	0.655	0.204	0.387	5.101	1.345
5^3A_u	6.909	0.000	0.000	-	-	5.129	1.429
7^1A_g	7.126	0.000	0.389	0.139	-0.118	4.918	1.438
8^1A_g	7.142	0.000	0.254	0.001	-0.003	3.271	1.364
6^3A_u	7.260	0.000	0.000	-	-	4.953	1.651
6^1A_u	7.356	0.000	0.211	-0.001	-0.003	3.290	1.442

Table S5: States of B for geometry at $\theta = 90°$: vertical excitation energies (ΔE, eV), oscillator strengths (f) and wave function descriptors. All B states are high in energy

$\theta = 90°$							
State	ΔE	f	Ω	P_{he}	R_{he}	$n_{u,nl}$	p
1^1B_g	4.704	0.000	0.000	-	-	4.473	1.164
1^1B_u	4.753	0.007	0.730	0.301	0.105	4.675	1.179
1^3B_u	4.787	0.000	0.728	0.111	0.057	4.653	1.305
1^3B_g	4.826	0.000	0.000	-	-	4.670	1.304
2^3B_g	4.899	0.000	0.000	-	-	4.729	1.318
2^1B_u	5.078	0.000	0.422	-0.004	0.011	2.249	1.315
2^1B_g	5.381	0.000	0.351	-0.005	0.009	2.278	1.369
3^1B_g	5.547	0.000	0.000	-	-	4.289	1.062
3^1B_u	5.979	0.000	0.437	-0.001	0.011	2.198	1.287
4^1B_g	6.143	0.000	0.370	0.004	0.009	2.201	1.294
4^1B_u	6.565	0.701	0.902	-0.428	0.046	4.522	1.188
5^1B_u	7.286	0.000	0.000	-	-	5.242	1.422
2^3B_u	7.392	0.000	0.000	-	-	5.302	1.562
5^1B_g	8.297	0.000	0.408	0.038	-0.173	5.182	1.608
6^1B_g	9.812	0.000	0.136	-0.407	0.364	5.097	1.883
6^1B_u	10.116	0.000	0.000	-	-	6.417	2.089

S5 – Output of configurations in MS-CASPT2 computations.

Table S6: Prominent configurations and their weights for the planar geometry of pQDM computed at the MS-CASPT2 level of theory. Only the configurations with weights above 15% are presented.

$\theta = 0°$

State	CI weight	Configuration
1^1A_g	0.88	2 020 0 220
1^3A_u	0.81	2 u20 0 2u0
1^3A_g	0.31	2 020 0 2uu
	0.44	2 uu0 0 220
1^1A_u	0.85	2 u20 0 2d0
2^1A_g	0.30	2 220 0 200
	0.27	2 ud0 0 220
	0.18	2 020 0 2ud
2^3A_u	Highly mixed state	
2^3A_g	0.47	2 020 0 2uu
	0.37	2 uu0 0 220
3^3A_u	0.19	2 2u0 0 2u0
	0.17	2 u20 0 20u
3^1A_g	0.29	2 ud0 0 220
	0.53	2 020 0 2ud
4^1A_g	0.20	2 220 0 200
	0.18	2 ud0 0 220
2^1A_u	0.29	2 u20 0 d20
3^1A_u	Highly mixed state	
3^3A_g	0.30	u d20 u 2u0
4^3A_u	0.25	2 u20 0 u20
5^1A_g	Highly mixed state	

Table S7: Prominent configurations and their weights for selected states of pQDM at twisted geometry computed at the MS-CASPT2 level of theory. Only the configurations with weights above 15% are presented.

$\theta = 90°$

State	CI weight	Configuration
1^1A_g	0.47	2 220 0 200
	0.40	2 020 0 220
1^3A_u	0.87	2 u20 0 2u0
2^1A_g	0.64	2 ud0 0 2ud
	0.21	2 uu0 0 2dd
1^3A_g	0.42	2 ud0 0 2uu
	0.29	2 uu0 0 2ud
2^3A_u	0.44	2 2u0 0 20u
	0.40	2 0u0 0 22u
1^1A_u	0.84	2 2u0 0 2d0
3^3A_u	0.84	2 2u0 0 2u0
3^1A_g	0.82	2 ud0 0 220
2^3A_g	0.83	2 uu0 0 220
4^1A_g	0.35	2 220 0 200
	0.40	2 020 0 220
2^1A_u	0.15	2 2u0 0 20d
	0.72	2 u20 0 2d0
3^1A_u	0.85	2 u20 0 20d
5^1A_g	0.84	2 020 0 2ud

S6 – Potential curves

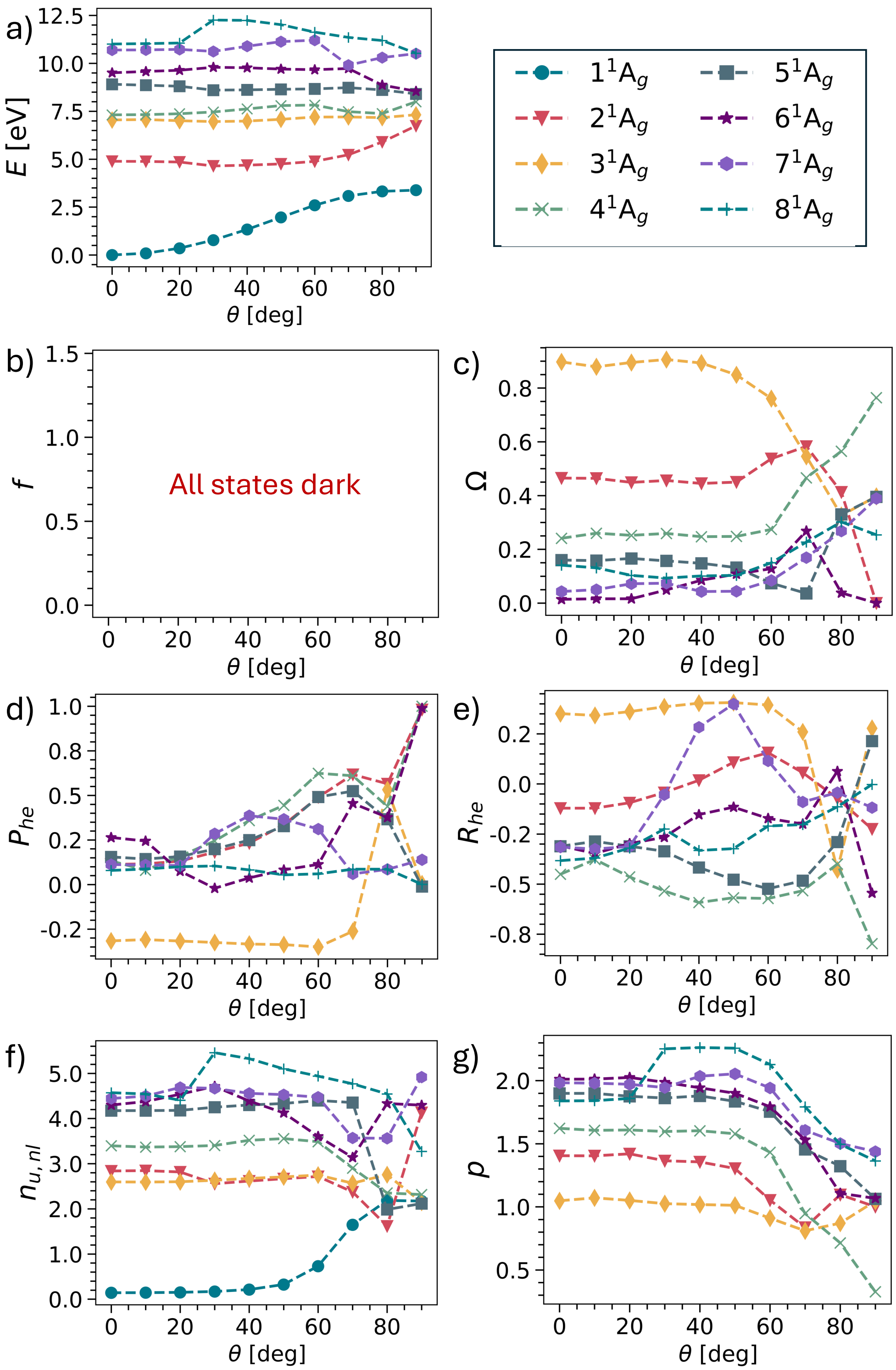

Figure S2: Potential curve of pQDM with change of the torsional angle, θ. Singlets of A_g symmetry are presented.

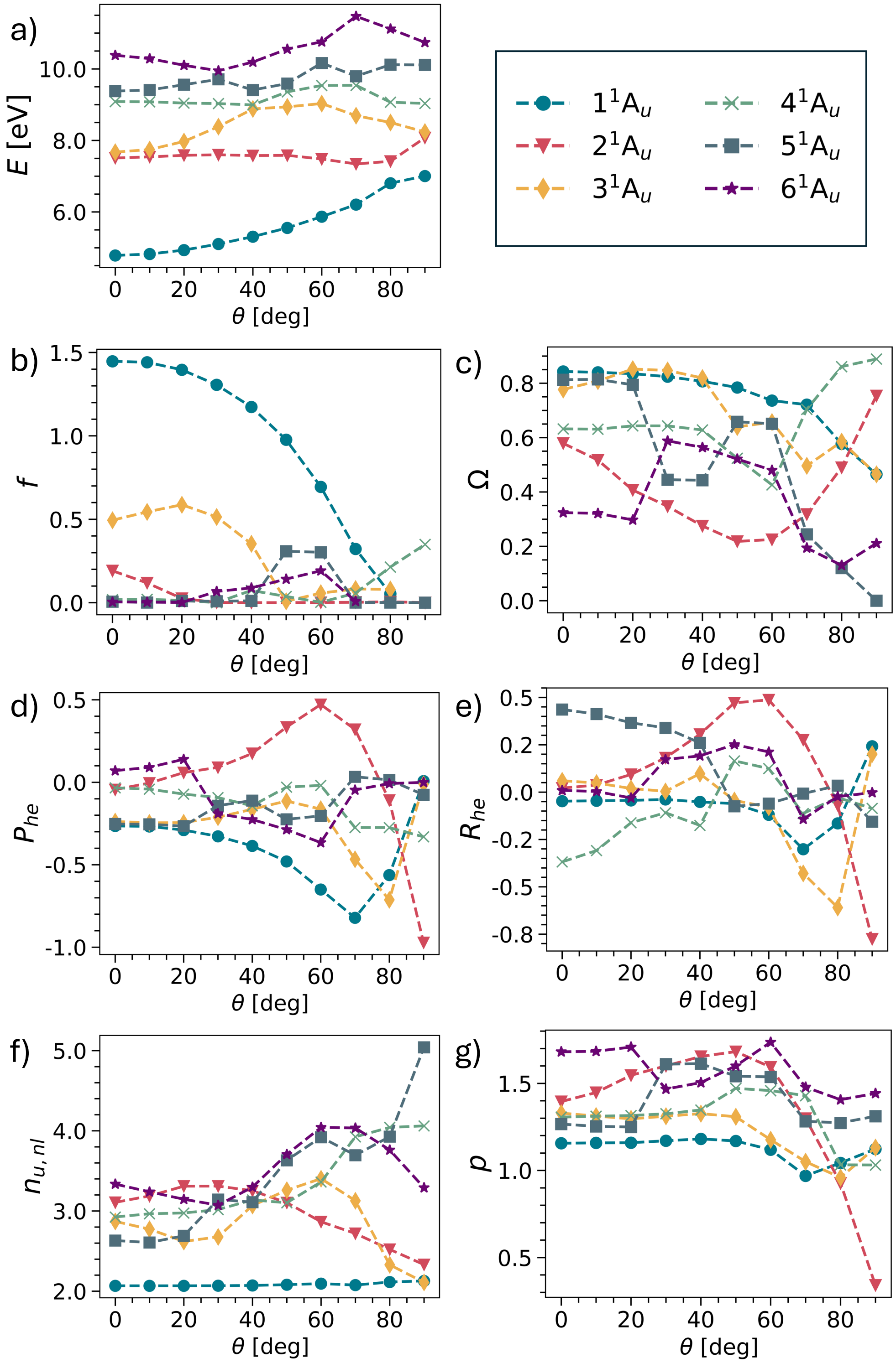

Figure S3: Potential curve of pQDM with change of the torsional angle, θ. Singlets of A_u symmetry are presented.

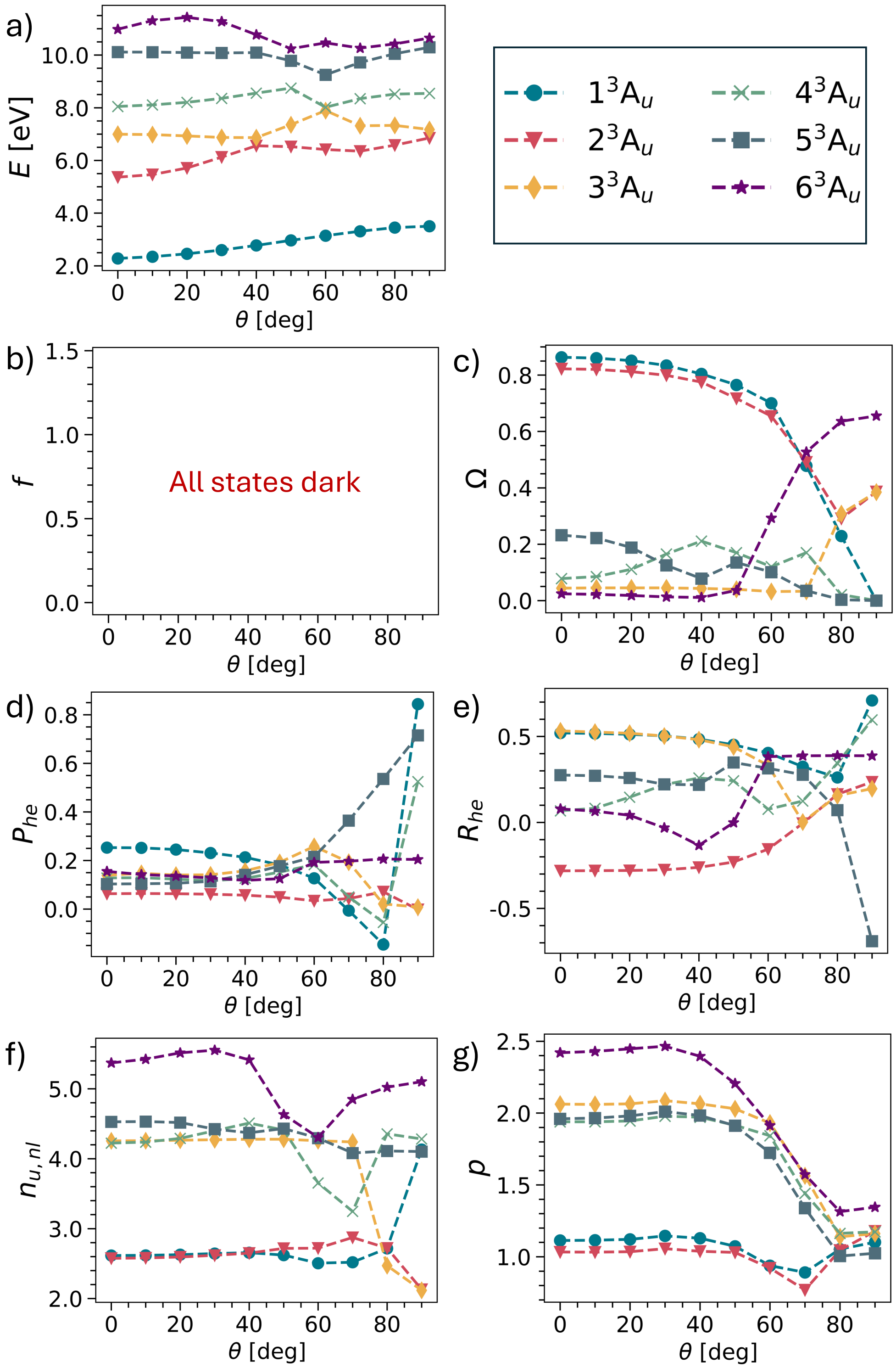

Figure S4: Potential curve of pQDM with change of the torsional angle, θ. Triplets of A_g symmetry are presented.

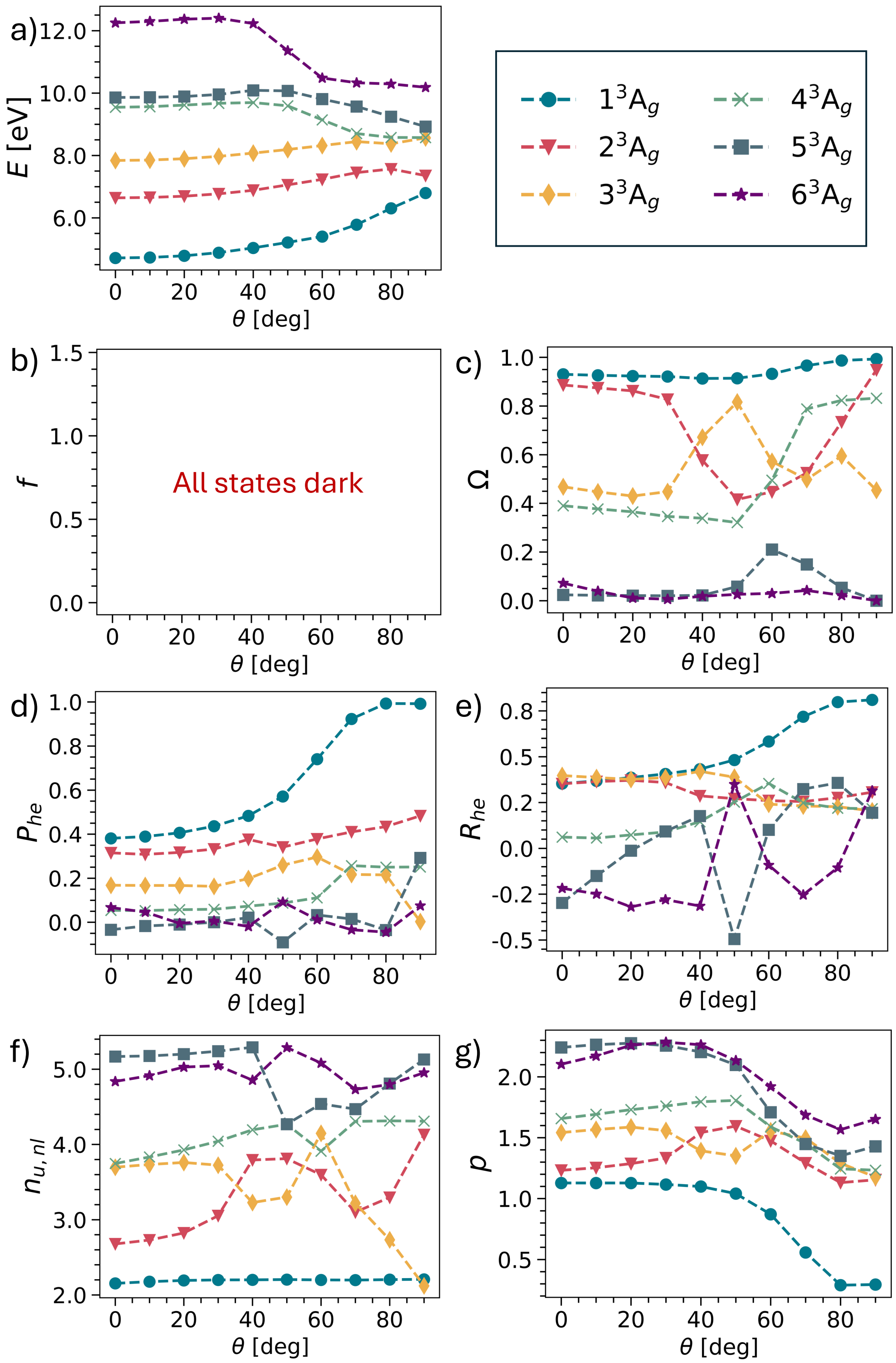

Figure S5: Potential curve of pQDM with change of the torsional angle, θ. Triplets of A_u symmetry are presented.